© 2016. Published by The Company of Biologists Ltd | Development (2016) 143, 3119-3127 doi:10.1242/dev.141226

RESEARCH ARTICLE

Cyclin CYB-3 controls both S-phase and mitosis and is asymmetrically distributed in the early *C. elegans* embryo

W. Matthew Michael*

ABSTRACT

In early *C. elegans* embryos the timing of cell division is both invariant and developmentally regulated, yet how the cell cycle is controlled in the embryo and how cell cycle timing impacts early development remain important, unanswered questions. Here, I focus on the cyclin B3 ortholog CYB-3, and show that this cyclin has the unusual property of controlling both the timely progression through S-phase and mitotic entry, suggesting that CYB-3 is both an S-phase-promoting and mitosis-promoting factor. Furthermore, I find that CYB-3 is asymmetrically distributed in the two-cell embryo, such that the somatic precursor AB cell contains ~2.5-fold more CYB-3 than its sister cell, the germline progenitor P_1. CYB-3 is not only physically limited in P_1 but also functionally limited, and this asymmetry is controlled by the *par* polarity network. These findings highlight the importance of the CYB-3 B3-type cyclin in cell cycle regulation in the early embryo and suggest that CYB-3 asymmetry helps establish the well-documented cell cycle asynchrony that occurs during cell division within the P-lineage.

KEY WORDS: *Caenorhabditis elegans*, Early embryo, Cell cycle, CYB-3 cyclin, Asynchrony, DNA replication

INTRODUCTION

How cell cycle control pathways are regulated during early embryogenesis and the means by which cell cycle timing impacts development are important and open research questions that span the fields of cell and developmental biology. The early *C. elegans* embryo is particularly well suited to address these problems as it is amendable to both cytological and genetic analysis, and these attributes have allowed multiple large-scale efforts that have revealed the genes, protein-protein interactions and molecular machineries required for cell division in the early embryo (Fraser et al., 2000; Gönczy, et al., 2000; Kamath et al., 2003; Gunsalus et al., 2005; Sönnichsen et al., 2005; Boxem et al., 2008). Despite these advantages, however, we still only have a rudimentary understanding of how the cell cycle is regulated in the early *C. elegans* embryo and thus further efforts are required if we are to achieve a systems-level understanding of this crucial process.

The first mitotic cycle in the early embryo is initiated shortly after fertilization and the completion of meiosis. Sperm entry triggers the maternal pronucleus to complete meiotic divisions and both the maternal and paternal pronuclei then initiate DNA replication (Edgar and McGhee, 1988; Sonneville et al., 2012). As replication is finishing, the maternal pronucleus begins to migrate across the embryo where it eventually meets with the paternal pronucleus (pronuclear meeting, or PNM), which is positioned at the future posterior side of the embryo. The two pronuclei then move towards the embryo center in a process termed pronuclear centration (PNC), where they remain prior to nuclear envelope breakdown (NEB) and entry into mitosis. Interphase of the first cell cycle can thus be divided into two portions: S-phase takes about half the time and is complete by the time of PNM (Sonneville et al., 2012, 2015); and the second half is composed of a G2/prophase period when nuclei display highly condensed chromosomes and an intact nuclear envelope. Key developmental events are also occurring during the first cell cycle as the embryo becomes polarized along its anterior-posterior axis. Polarization is directed by the *par* network and results in asymmetric cleavage, whereby the zygote divides to form the larger AB and smaller P_1 cell (reviewed by Rose and Gönczy, 2014).

Polarization of the zygote produces numerous asymmetries in the early embryo that are important for both cell fate acquisition and cell cycle remodeling after the first division. For example, polarity promotes the asymmetric distribution of germ cell determinants to the germline precursor P_1 cell and their clearance from the somatic AB cell (Rose and Gönczy, 2014). Polarity also promotes cell cycle remodeling – the G2 phase is lost in both AB and P_1 as these cells lack gap phases altogether and transit directly into S-phase and then mitosis (Edgar and McGhee, 1988). In addition, AB and P_1 inherit different cell cycle timing programs; the P_1 S-phase is invariably 2 min longer than the AB S-phase (reviewed by Tavernier et al., 2015). This S-phase asynchrony continues, and is extended, within the P-lineage, as the P_1 descendants P_2, P_3 and P_4 all have progressively longer S-phases than their somatic sister cells. S-phase asynchrony is controlled by the *par* network and be can be partially uncoupled from asymmetric cleavage, as mutations in two genes, *par-1* and *par-4*, retain asymmetric cleavages while S-phase asynchrony is lost (Kemphues et al., 1988; Morton et al., 1992). Whether S-phase asynchrony in P-cells is important for germline specification is not known.

Cdk-cyclin complexes provide cells with both S-phase-promoting factor (SPF) and mitosis-promoting factor (MPF) activities. In metazoans, SPFs are typically composed of Cdk2 bound to either cyclins E or A, while MPFs are Cdk1 bound to A- and B-type cyclins (reviewed by Fisher, 2011; Siddiqui et al., 2013; Wieser and Pines, 2015). In some embryonic systems, however, it might be the case that both SPF and MPF contain Cdk1 (Farrell et al., 2012), and Cdk1 can perform both functions in mammalian cells that have lost Cdk2 (Ortega et al., 2003). In *C. elegans* embryos, the SPF is not known and MPF activity is provided by CDK-1 bound to either CYB-1 (a cyclin B) or CYB-3 (a cyclin B3) (van der Voet et al., 2009). CYB-1 and CYB-3 have both redundant and distinct functions during the early cell cycles. Depletion of CYB-1 causes a modest delay in NEB and a profound defect in

Molecular and Computational Biology Section, Department of Biological Sciences, University of Southern California, Los Angeles, CA 90089, USA.

*Author for correspondence (mattm@usc.edu)

W.M.M., 0000-0002-8535-5796

Received 16 June 2016; Accepted 21 July 2016

Development (2016) 143, 3119-3127 doi:10.1242/dev.141226

chromosome congression to the metaphase plate (van der Voet et al., 2009). Depletion of CYB-3 causes a more severe delay in NEB, and cells then arrest at metaphase (Cowan and Hyman, 2006; van der Voet et al., 2009; Deyter et al., 2010). Thus, as is the case for cyclin B3 proteins in other organisms (Yuan and O'Farrell, 2015; Zhang et al., 2015), CYB-3 is required to promote anaphase. Interestingly, work in *C. elegans* has revealed additional functions for CYB-3 prior to mitotic entry (Deyter et al., 2010). In *cyb-3 (RNAi)* zygotes, interphase events such as chromosome condensation, pronuclear migration and centrosome maturation are all delayed, suggesting that CYB-3 has important interphase functions in addition to a role in mitosis. To date, CYB-1 and CYB-3 are the only cyclins known to have a major role in cell cycle progression in the early embryo. Two other cyclin B orthologs, the highly related CYB-2.1 and CYB-2.2 proteins, are not essential for viability nor are they required for proper cell cycle timing in early embryos (Rabilotta et al., 2015). Loss of a cyclin A ortholog, CYA-1, causes late embryonic lethality whereas early embryogenesis occurs normally (Yan et al., 2013). Furthermore, previous work has examined loss of *cdk-2* and *cye-1* (cyclin E) in the early embryo (Cowan and Hyman, 2006), and although a minor cell cycle delay was observed there were no obvious defects in either DNA replication or centrosome duplication.

In this study I further explore CYB-3 function during the early cell cycles in *C. elegans* embryos. I observe that loss of CYB-3 causes delays in both S-phase progression and mitotic entry in one-cell embryos, suggesting that this single cyclin might contain both SPF and MPF activities. In addition, I report that at the two-cell stage CYB-3 is asymmetrically distributed in a *par*-dependent manner, such that AB contains ~2.5-fold more CYB-3 than does P_1. Furthermore, CYB-3 is not only physically limited in P_1 relative to AB, but is also functionally limited. These data provide new insight into how the cell cycle is regulated during early embryogenesis and also suggest a new model for how S-phase asynchrony is achieved in the early embryo.

RESULTS

CYB-3 is required for timely DNA replication

Previous findings have linked CYB-3 to DNA replication in *C. elegans* embryos. For example, it was recently shown that chromosome condensation is dependent on DNA replication (Sonneville et al., 2015), and previous work has shown that condensation is delayed in *cyb-3(RNAi)* embryos (Deyter et al., 2010). In addition, the canonical metazoan SPF, Cdk2-cyclin E, is dispensable for replication in early embryos (Cowan and Hyman, 2006), suggesting that an atypical SPF is involved. I therefore asked if CYB-3 plays a role in DNA replication.

Replication was analyzed by immunostaining fixed embryos with an antibody raised against PCN-1, the worm ortholog of the replication fork protein PCNA. This antibody recognizes a single major band of the appropriate size on western blots of early embryos (Fig. S1A). Wild-type one-cell embryos were examined first, and these could be staged temporally by the position of the pronuclei (Fig. 1A). Early embryos contain well-separated pronuclei (Fig. 1Ai), in older embryos the maternal pronucleus migrates (Fig. 1Aii), then meets the paternal pronucleus (PNM; Fig. 1Aiii), and finally the two pronuclei assume the central position (PNC; Fig. 1Aiv). In wild-type embryos, a bright PCN-1 signal was observed in early embryos, where both the maternal and paternal pronuclei were intensely stained (Fig. 1Bi). In contrast to early one-cell embryos, little or no PCN-1 signal was observed in older mid-migration embryos, or in even older PNM or PNC embryos (Fig. 1Bii-iv).

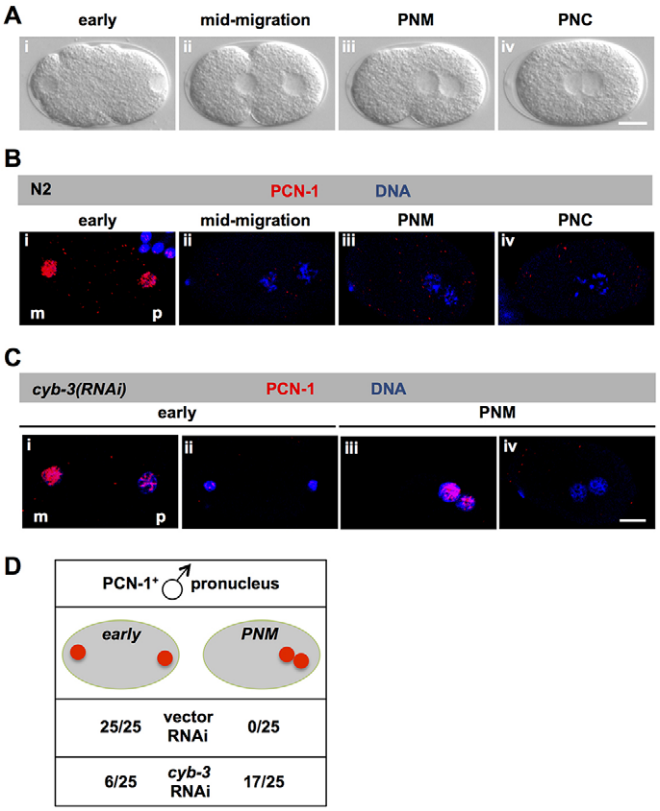

Fig. 1. CYB-3 is required for timely DNA replication in early *C. elegans* embryos. (A) Time-lapse DIC images of a single embryo progressing through the first mitotic cycle. The developmental stage of the embryo is indicated. PNM, pronuclear meeting; PNC, pronuclear centration. (B) Early wild-type embryos were fixed and immunostained for PCN-1 (red) and stained with DAPI to visualize the DNA (blue). Panels are organized as in A. Maternal (m) and paternal (p) pronuclei are labeled in Bi. (C) Same as in B except that embryos were obtained from *cyb-3(RNAi)* mothers and two examples each of early and PNM embryos are shown. (D) Quantification of PCN-1 signal distribution in the paternal pronucleus for vector RNAi control and *cyb-3(RNAi)* samples. Data shown are from a single experiment and are representative of two independent biological replicates. Scale bars: 10 µm.

Importantly, previous work had examined replication kinetics in one-cell embryos using live cell imaging and a GFP-tagged CDC-45 protein, a marker for the presence of active replication forks (Sonneville et al., 2012, 2015). This work demonstrated that replication initiates in both pronuclei very shortly after the completion of meiosis, and that replication is complete prior to the PNM stage. Data shown in Fig. 1B are in excellent agreement with these previous studies. Furthermore, as detailed in Fig. S1B, PCN-1 staining of two- and four-cell embryos also gave the expected pattern whereby nuclei are PCN-1 positive only if they are in S-phase. Based on the data in Fig. 1B and Fig. S1B, I conclude that PCN-1 immunostaining is a reliable method to mark actively replicating nuclei in early embryos.

To examine the impact of CYB-3 depletion on DNA replication, I used RNAi to reduce CYB-3 levels. As detailed in the supplementary Materials and Methods, our RNAi targeting construct is expected to be specific for *cyb-3* and not co-deplete other *cyb* gene products. The RNAi conditions were effective, as assessed by the high (100%) embryonic lethality in the progeny of fed mothers (Fig. S2A). To examine replication, control or *cyb-3(RNAi)* embryos were fixed and stained for PCN-1 (Fig. 1C,D). The control RNAi samples were highly similar to the samples shown in Fig. 1B, as expected

Development (2016) 143, 3119-3127 doi:10.1242/dev.141226

(summarized in Fig. 1D). By contrast, *cyb-3(RNAi)* embryos revealed a very different pattern. In many embryos, there was as an imbalance between the maternal and paternal pronuclei, such that the PCN-1 signal was more intense in the maternal pronucleus (Fig. 1Ci).

Because CYB-3 is required for the proper completion of meiotic anaphase II, polar body extrusion often fails in *cyb-3(RNAi)* embryos (van der Voet et al., 2009; Deyter et al., 2010), and this can result in diploid maternal pronuclei. Thus, from embryo to embryo, *cyb-3* RNAi produces maternal pronuclei of varying DNA content, and this complicates the analysis of replication. To avoid this I focused solely on the PCN-1 signal status of the paternal pronucleus, the DNA content of which is unlikely to be affected by *cyb-3* RNAi. Embryos were scored for the presence or absence of PCN-1 signal in the paternal pronucleus of early embryos. Results showed that 6 out of 25 early embryos displayed a PCN-1 signal in the paternal pronucleus, but it was often weak (Fig. 1Ci,D). Importantly, the majority of early embryos (19/25) displayed no detectable PCN-1 signal in the paternal pronucleus, and these embryos often lacked a signal in the maternal pronucleus as well (Fig. 1Cii,D). This was in contrast to wild-type samples, where PCN-1 signal was always observed in early embryos (Fig. 1D). Older *cyb-3(RNAi)* embryos, at the PNM stage, were also examined, and in these the PCN-1 signal was present in the majority (17/25) of the samples examined (Fig. 1Ciii,iv,D). PCN-1-positive PNM embryos were not observed in the wild type (Fig. 1D).

These data show that DNA replication is delayed after CYB-3 depletion: replication does not occur efficiently in early samples but is observed in older samples, whereas wild-type samples show the reciprocal pattern (Fig. 1D). I note that previous work has shown that maternal pronuclear migration is delayed in *cyb-3(RNAi)* embryos (Deyter et al., 2010), and despite this I still observe replicating nuclei at the PNM stage in these embryos. This underscores the delay in DNA synthesis that occurs in *cyb-3 (RNAi)* embryos, and I thus conclude that CYB-3 is required for the timely progression through S-phase in early embryos.

Data in Fig. 1 show a DNA replication function for CYB-3. Interestingly, previous work had shown that *cyb-3(RNAi)* embryos are delayed for mitotic entry at the one-cell stage (Cowan and Hyman, 2006; van der Voet et al., 2009; Deyter et al., 2010), and this could be due to a requirement for CYB-3 in initiating mitosis (i.e. NEB), or to a checkpoint-mediated delay in mitotic entry because of problems in DNA replication, or both. To examine this more closely, I asked if co-inactivation of the replication checkpoint would affect the interphase delay imposed by depletion of *cyb-3*. Previous work has established that replication stress, as imposed by depletion of replication fork components or limitation of dNTP supplies, delays interphase in one-cell embryos and that depletion of the checkpoint components ATL-1 (ATR kinase) and CHK-1 (Chk1 kinase) reverses the delay (Brauchle et al., 2003). I measured cell cycle timing in embryos depleted of *cyb-3* and compared them with embryos that had been triply depleted of *cyb-3*, *atl-1* and *chk-1*. Timing was performed as described (Sonneville et al., 2015), whereby the elapsed time between the PNM stage and NEB was recorded for each sample (Fig. 2A). Timing of a partial cell cycle is necessary at the one-cell stage as events occurring just after fertilization are difficult to visualize with differential interference contrast (DIC) microscopy (see Brauchle et al., 2003).

As shown in Fig. 2B, *cyb-3(RNAi)* embryos were delayed for mitotic entry, relative to the control samples. By contrast, *atl-1/chk-1(RNAi)* embryos showed faster cell cycle progression relative to control samples, which is consistent with previous results (Brauchle et al., 2003) and demonstrates efficacy of the RNAi. The triply depleted samples resembled those in which *cyb-3* alone had been depleted (Fig. 2B), showing that loss of ATL-1/CHK-1 activity has no effect on the interphase delay in *cyb-3(RNAi)* embryos. These data show that CYB-3 directly controls mitotic entry, independent of its role in promoting timely S-phase completion.

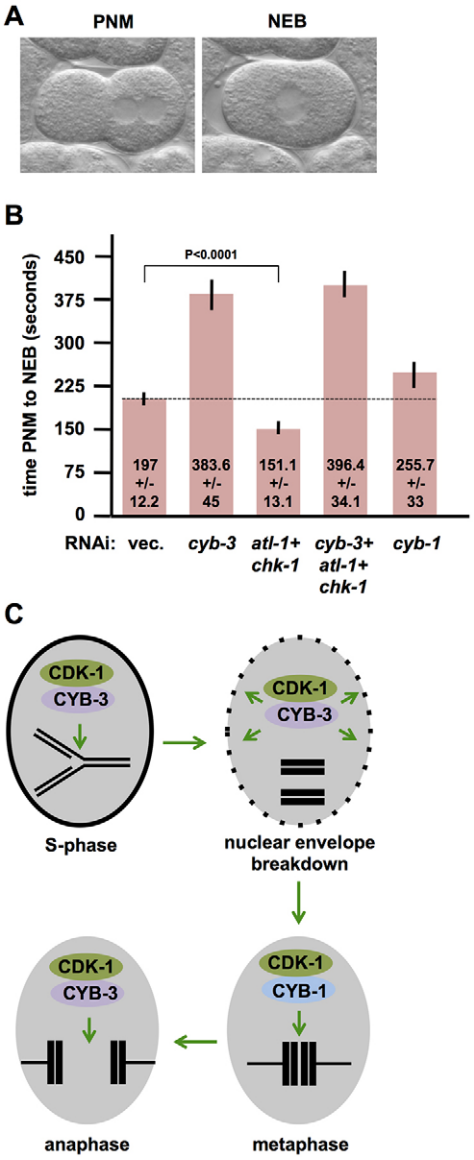

Fig. 2. Inactivation of *cyb-3* delays interphase progression in a replication checkpoint-independent manner. (A) Time-lapse DIC images of a single embryo progressing from the PNM stage to NEB are shown to indicate how the timing data in B were collected. (B) Ten embryos per genotype were timed as depicted in A and the data were averaged and plotted. Samples were analyzed in groups of five, the experiment was performed twice, and the values were then combined. Error bars indicate s.d.; *P*-value determined by Student's *t*-test. (C) Model depicting the division of labor for CYB-1 and CYB-3 during the early embryonic cell cycle. In this model, CYB-3 drives the early events (DNA replication and NEB), CYB-1 controls chromosome attachment to the metaphase plate, and CYB-3 then promotes anaphase.

To pursue these observations, and to gain insight into the role of CYB-1 in promoting NEB, I also timed *cyb-1(RNAi)* embryos. Data showed that CYB-1 depletion caused only a modest delay in NEB (Fig. 2B), suggesting that CYB-3 plays the dominant role in promoting NEB. The *cyb-1* RNAi was effective, as assessed by the high degree of embryonic lethality observed (87.3%; Fig. S2A).

Development (2016) 143, 3119-3127 doi:10.1242/dev.141226

Taken together, the data shown in Figs 1 and 2 suggest a model for how CYB-1 and CYB-3 function together to mediate cell cycle progression (Fig. 2C). I propose that CYB-3 plays the major role in promoting both S-phase progression and NEB, whereas CYB-1 plays a less prominent role in these events. At metaphase, CYB-1 plays the major role in ensuring proper alignment of chromosomes to the metaphase plate (van der Voet et al., 2009), and at anaphase CYB-3 plays a major role in allowing anaphase onset (Deyter et al., 2010). As proposed by the model, our data, together with previous results, suggest that the early embryonic cell cycle in *C. elegans* is primarily driven by B-type cyclins. Although further work is needed to validate this model, it is clear that B-type cyclins assume a wider range of functions in the early worm embryo than is typically encountered in a metazoan cell cycle.

Localization of CYB-3 in one-cell and two-cell embryos

To pursue the function of CYB-3 during S-phase in early embryos I required detailed information about its subcellular localization and intra-embryo distribution at the one- and two-cell stages. Previous work has reported an antibody specific for CYB-3 (van der Voet et al., 2009), but this antibody is no longer available. A GFP-tagged transgene was considered, but such fusions with CYB-1 have been produced and are non-functional in early embryos; more specifically, GFP-CYB-1 can be detected in oocytes and fertilized embryos undergoing meiosis but it disappears after meiosis and does not reappear during the mitotic cell cycles (Liu et al., 2004, McNally and McNally, 2005; Wang et al., 2013; W.M.M., unpublished observations). Given that a GFP-CYB-3 fusion would be likely to behave in a similar manner, an alternative approach was sought to localize CYB-3 within the embryo. Previous work has utilized the monoclonal antibody (Mab) F2F4, produced against *Drosophila* Cyclin B, to detect a B-type cyclin in *C. elegans* (Shakes et al., 2009; Rahman et al., 2014), although the specificity of this Mab had not yet been examined. As detailed in the supplementary Materials and Methods and Fig. S2B,C, it was determined that Mab F2F4 recognizes CYB-3. Staining of one-cell embryos with Mab F2F4 revealed a nuclear signal in early, mid-migration, and PNC embryos (Fig. 3A-C), as expected based on previous results (van der Voet et al., 2009; Rahman et al., 2014). I note that previous work using either the antibodies raised against CYB-3 (van der Voet et al., 2009) or Mab F2F4 (Rahman et al., 2014) showed a weak cytoplasmic signal in addition to a prominent nuclear signal, whereas in our experiments the cytoplasmic signal was difficult to detect whereas the nuclear signal was very strong (Fig. 3A-C). The reason for this discrepancy is unknown, but is likely to be linked to differences in the fixation protocols utilized here versus the previous studies.

I next examined CYB-3 localization at the two-cell stage. For this analysis it was also important to detect P-CDK-1, which is the tyrosine 15-phosphorylated and inhibited form of the enzyme. Tyrosine phosphorylation of Cdk-cyclin B complexes is required during S-phase to restrain mitotic entry until replication has finished (Wieser and Pines, 2015). I used a commercially available antibody raised against human P-CDK-1 for this analysis. Similar human P-

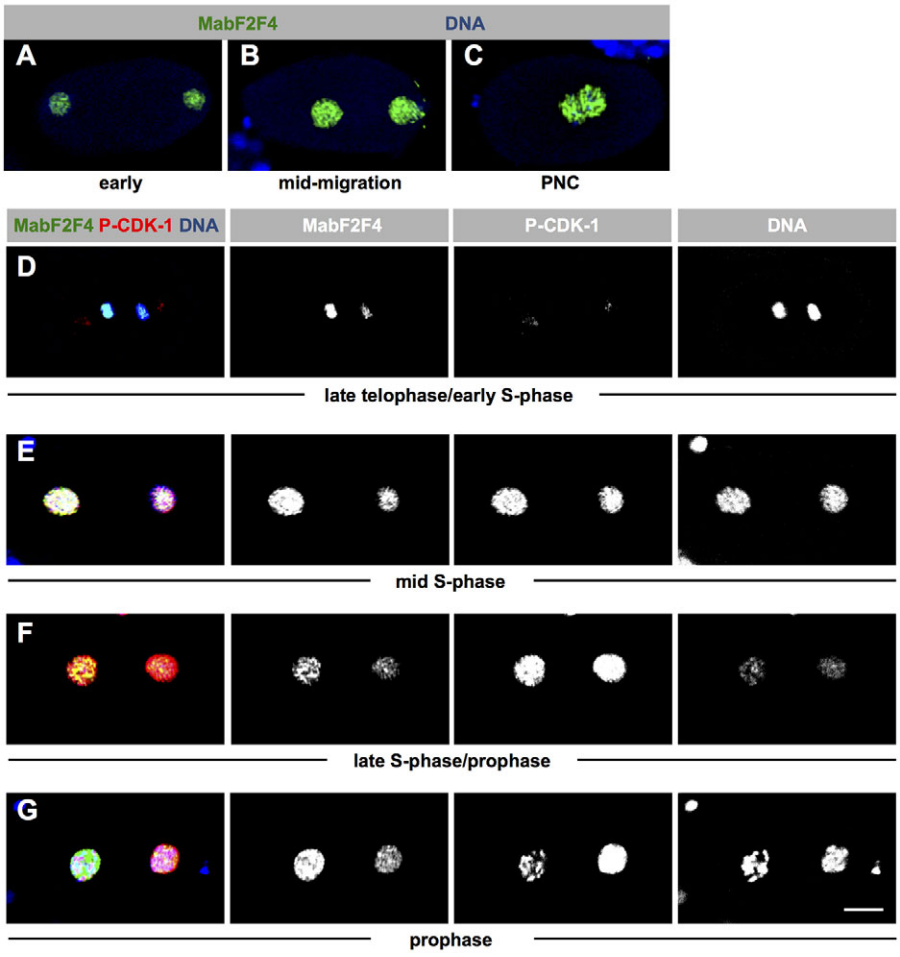

Fig. 3. Subcellular localization of CYB-3 in early embryos. (A-C) One-cell embryos from the indicated stages were fixed and stained with Mab F2F4 (green) and DAPI (blue) to visualize CYB-3 and DNA, respectively. (D-G) Two-cell embryos were fixed and stained for CYB-3 (Mab F2F4, green), P-CDK-1 (red) and DNA (DAPI, blue). Anterior, and thus AB, is to the left in all panels. The first column shows simultaneous detection of all three signals; the remaining columns show the individual signals. D depicts a very early two-cell embryo; E-G depict progressively later interphase embryos. Scale bar: 10 µm.

Development (2016) 143, 3119-3127 doi:10.1242/dev.141226

CDK-1 antibodies have been successfully used to detect P-CDK-1 in *C. elegans* embryos (Hachet et al., 2007; Rahman et al., 2014), and I found that this antibody is specific for *C. elegans* P-CDK-1 (see the supplementary Materials and Methods and Fig. S3).

Mab F2F4 and anti-P-CDK-1 were used to co-stain fixed embryos to detect CYB-3 and P-CDK-1, respectively (Fig. 3D-G). CYB-3 protein was localized to the nucleus whenever it was present, even in late telophase/early S-phase embryos (Fig. 3D). The nuclear signal persisted during S-phase and into prophase (Fig. 3E-G), which is consistent with what occurs in one-cell embryos (Fig. 3A-C). A striking feature of the CYB-3 localization pattern in two-cell embryos is that, throughout interphase, it is asymmetrically distributed such that AB contains more CYB-3 than P_1 (Fig. 3D-G). Importantly, this is the case even in very early two-cell embryos (Fig. 3D). This asymmetric distribution is analyzed in more detail below. Regarding the P-CDK-1 pattern, in very early two-cell embryos P-CDK-1 was not detected within nuclei (Fig. 3D), whereas in older embryos nuclear P-CDK-1 was readily detected (Fig. 3E-G). In some two-cell embryos, namely those that were in early S-phase as inferred by nuclear size and position as well as chromosome morphology, there appeared to be slightly more P-CDK-1 in AB relative to P_1 (see Fig. 3E). In older two-cell embryos, the P-CDK-1 signal evened out and then became more pronounced in P_1 relative to AB (Fig. 3F,G).

The data in Fig. 3 make two important points. First, CYB-3 is asymmetrically distributed in two-cell embryos. Second, CYB-3 protein is present in nuclei during late telophase/early S-phase, whereas P-CDK-1 is not (Fig. 3D). This suggests that CDK-1–CYB-3 complexes are active in very early S-phase, and then inactivated via inhibitory phosphorylation at some point later in S-phase, and thus that a window of opportunity exists during which CDK-1–CYB-3 can promote S-phase prior to inhibition. It is not yet known if the CYB-3 present during late telophase/early S-phase represents newly synthesized protein or protein that escaped degradation during the preceding mitosis.

PAR-1 and PAR-4 are required for the asymmetric distribution of CYB-3

Data shown thus far reveal that CYB-3 is less abundant in P_1 relative to AB (Fig. 3). I next determined if this asymmetric distribution of CYB-3 is under genetic control. *par-1* and *par-4* were examined since both control S-phase asynchrony in two-cell embryos (Kemphues et al., 1988; Benkemoun et al., 2014). Consistent with Fig. 3, CYB-3 was asymmetrically distributed in wild-type two-cell embryos (Fig. 4Ai), with ∼2.5-fold more CYB-3 in AB than P_1 (Fig. 4B). Importantly, the asymmetric distribution was compromised in *par-1* and *par-4* mutant embryos (Fig. 4Aii,iii,B). CYB-3 was evenly distributed in *par-4* mutants and the imbalance in CYB-3 levels between AB and P_1 was greatly diminished in *par-1* mutants. These data show that the asymmetric distribution of CYB-3 is likely to be controlled by polarity cues dependent on *par* genes, as is S-phase asynchrony.

CYB-3 activity is limiting in P_1 relative to AB

Data shown thus far indicate that CYB-3 promotes timely DNA replication and is asymmetrically distributed in two-cell embryos, such that the cell that finishes S-phase first (AB) contains more CYB-3 than its slower sister cell P_1. These data suggest that CYB-3 function might be limiting in P_1, relative to AB, under normal conditions. To pursue this possibility, I reasoned that if CYB-3 is limiting in P_1 then a reduction in CYB-3 levels should increase cell cycle timing in two-cell embryos in a manner whereby P_1 is impacted more than AB. I avoided using RNAi to reduce CYB-3 levels, as problems occurring prior to the two-cell stage would make the results difficult to interpret. Therefore, AB and P_1 timing was measured in embryos derived from mothers containing different copy numbers of the *cyb-3* gene. In two-cell embryos there is little if any zygotic transcription (Edgar et al., 1994), and thus all CYB-3 protein is derived from maternal sources. Accordingly, one would expect that the maternal *cyb-3* gene dosage would have direct effects on early embryonic cell cycle progression, as has been reported in *Drosophila* (Ji et al., 2004). The strains utilized for this analysis contain one (VC388; *cyb-3*$^{+/-}$) or two (N2; *cyb-3*$^{+/+}$) functional copies of the *cyb-3* gene. For VC388, only *cyb-3*$^{+/-}$ animals are fertile (see the supplementary Materials and Methods), and thus all embryos derived from VC388 mothers are 1X *cyb-3* with respect to the maternal contribution, whereas the wild-type N2 strain is 2X. Importantly, despite the reduction in *cyb-3* copy number, *cyb-3*$^{+/-}$ embryos derived from *cyb-3*$^{+/-}$ mothers are viable and fertile. Embryos were timed as described (Benkemoun et al., 2014), from the beginning of cortical ingression [arrows in Fig. 5A; this marks the onset of cytokinesis and telophase, which coincides with S-phase entry (Edgar and McGhee, 1988)] through to NEB in AB and P_1 (Fig. 5A).

Timing experiments revealed that both AB and P_1 cell cycles were significantly slower for VC388 than for N2 (Fig. 5B). Importantly, P_1-AB asynchrony was also significantly extended in VC388 embryos (Fig. 5C), from the typical ∼120 s to nearly 150 s. These data make it clear that even a modest reduction in CYB-3 levels can impact asynchrony at the two-cell stage. To determine if P_1 is more affected than AB by the reduction of CYB-3, I calculated the P_1/AB ratio (Fig. 5D). If the ratio increases then P_1 is impacted more than AB, whereas if the ratio decreases then the opposite is true

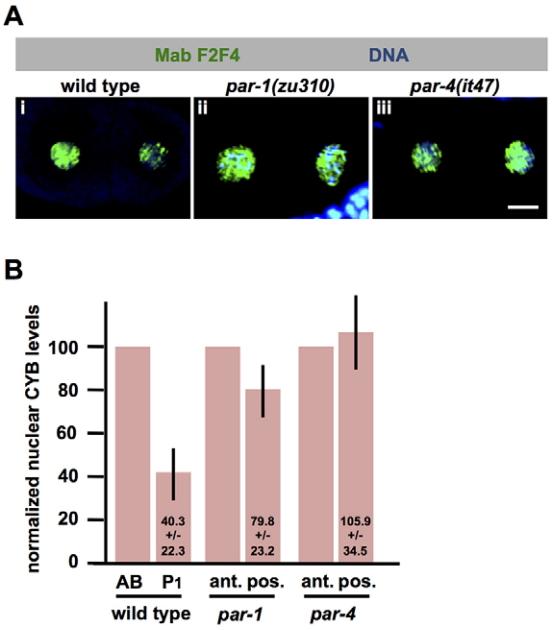

Fig. 4. The asymmetric distribution of CYB-3 is controlled by *par-1* and *par-4*. (A) Two-cell embryos of the indicated genotype were fixed and stained as in Fig. 3. Anterior is to the left. Scale bar: 10 µm. (B) Quantification of CYB-3 signal in two-cell embryos. Images captured from the experiment shown in A were quantified as described in the supplementary Materials and Methods. For each AB-P_1 pair, pixel intensity for the AB sample was set to 100 and P_1 values were adjusted accordingly. Data are derived from ten embryos per genotype; error bars indicate s.d. Data shown are from a single experiment and are representative of two independent biological replicates.

Development (2016) 143, 3119-3127 doi:10.1242/dev.141226

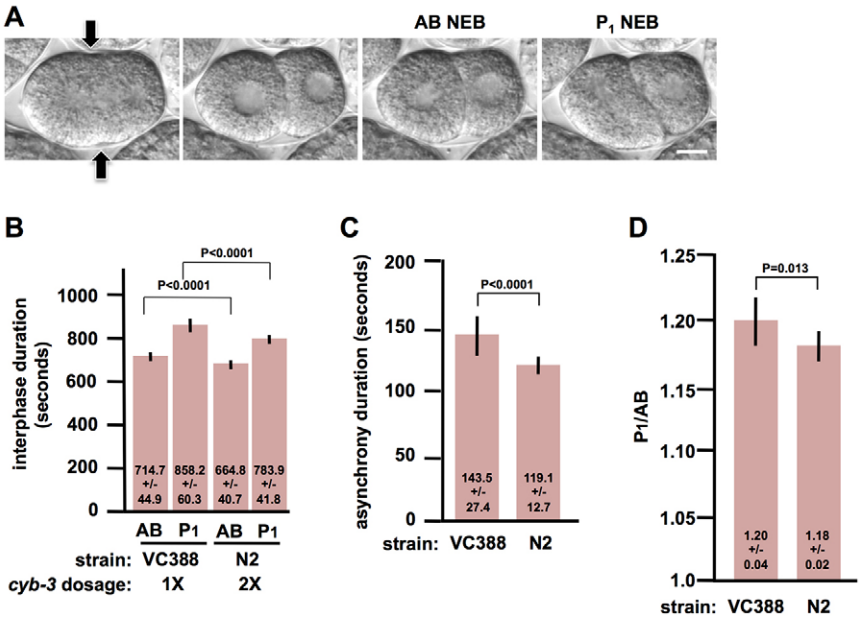

Fig. 5. CYB-3 activity is limiting in P_1 relative to AB. (A) Time-lapse DIC images of a single two-cell embryo progressing through the AB and P_1 cell cycles are shown to indicate how the timing data in B were collected. Arrows indicate cortical ingression, which is when timing was initiated. Timing was terminated at NEB. Scale bar: 10 µm. (B) Embryos derived from the indicated strain and of the indicated *cyb-3* copy number were timed for interphase duration. Data were collected from 30 N2 embryos and 31 VC388 embryos. Samples were analyzed in groups of 10 or 11, the experiment was performed three times, and the values were then combined. (C) Asynchrony determined for the samples shown in B. (D) The P_1/AB ratio for the samples shown in B. (B-D) Error bars indicate s.d.; *P*-values were determined by Student's *t*-test.

(Brauchle et al., 2003). For wild type, the P_1/AB ratio is 1.18, whereas for VC388 this ratio increased to 1.20 and the difference is significant (P=0.013, Student's *t*-test). These data show that a reduction in CYB-3 levels impacts P_1 more than AB, and thus that CYB-3 is both physically and functionally limiting in P_1 relative to AB.

The role of inhibitory phosphorylation of CDK-1 in cell cycle asynchrony

CDK-1–CYB-3 is required for S-phase progression (Fig. 1) and, independently, mitotic entry (Fig. 2). I have also shown that CYB-3 is both physically and functionally limiting in P_1 relative to AB (Figs 3–5). Thus, the CYB-3 asymmetry reported here could be a trigger for cell cycle asynchrony and, if so, it could be through either its presumptive SPF or MPF functions. I reasoned that if the SPF activity were responsible, then P-CDK-1 would play an important role in maintaining asynchrony, as this is the modification that allows differential DNA replication kinetics to be translated into differential cell cycle timing. By contrast, if the MPF activity were responsible, then the P-CDK-1 modification would be dispensable, because differential MPF levels would be expected to trigger differential mitotic entry, with or without the capacity to inhibit CDK-1 during replication. I therefore investigated the impact of P-CDK-1 on asynchrony in two-cell embryos.

Upon formation of Cdk1-cyclin B complexes, the catalytic Cdk1 subunit is phosphorylated and inhibited by Wee1/Myt1 (Wieser and Pines, 2015). Indeed, it is Wee1/Myt1-mediated phosphorylation of Cdk1 that is reinforced by the replication checkpoint during S-phase so that mitosis always follows a complete round of DNA replication (Wieser and Pines, 2015). I used RNAi to deplete the *Myt1* ortholog *wee-1.3*. Timing of these embryos revealed that interphase in both AB and P_1 was accelerated (Fig. 6A), and that P_1-AB asynchrony was reduced from ∼120 s to ∼65 s (Fig. 6B). This is a similar pattern to that previously observed for *atl-1/chk-1(RNAi)* embryos (Brauchle et al., 2003), and indeed I also observed accelerated interphase and reduced asynchrony after *atl-1/chk-1* RNAi (Fig. 6A,B). I next performed RNAi against all three genes, and observed in *wee-1.3/atl-1/chk-1(RNAi)* embryos that interphase acceleration was increased even further, and P_1-AB asynchrony was reduced even further, relative to the individual knockdowns (Fig. 6A,B). In these triply depleted embryos asynchrony was reduced to ∼43 s, which is a 64% reduction relative to wild type, and the P_1/AB ratio was also dramatically reduced from 1.17 to 1.08 (Fig. 6C). Based on these data, I conclude that inhibitory phosphorylation of CDK-1–CYB-3 plays a major role in maintaining cell cycle asynchrony at the two-cell stage.

DISCUSSION

Multiple roles for CYB-3 in early embryonic cell cycle progression

Work presented here, together with previous results, highlight the importance of the B3-type cyclin CYB-3 in early embryonic cell cycle progression in *C. elegans*. Previous work has shown that CYB-3 promotes timely mitotic entry, as assessed by time to NEB (Cowan and Hyman, 2006; van der Voet et al., 2009; Deyter et al., 2010), and I have shown here that it also promotes timely progression through S-phase (Fig. 1). Furthermore, I have shown that the mitotic delay observed upon CYB-3 depletion is not due to a checkpoint response to poor replication (Fig. 2), but rather reflects a direct role for CYB-3 in promoting NEB. It thus appears that CYB-3 functions continuously throughout the cell cycle, from S-phase entry to anaphase (Fig. 2C).

Our data reveal a DNA replication function for CYB-3, and this represents, to our knowledge, the first demonstration that a B3-type cyclin contains this activity. B3-type cyclins are a bit of an oddity in that, despite strong conservation of sequence and gene copy number within the metazoa, functional studies have yet to resolve a common function for the protein in cell cycle control (Lozano et al., 2012). Cyclin B3 proteins are always constitutively nuclear, but their preferred CDK binding partners show variation. Human cyclin B3 binds CDK2 but not CDK1 (Nguyen et al., 2002), the *Drosophila* protein binds CDK1 but not CDK2 (Jacobs et al., 1998), and chicken B3 binds both CDK1 and CDK2 (Gallant and Nigg, 1994). Worm CYB-3 binds CDK-1 (van der Voet et al., 2009), but whether it also binds CDK-2 has not been examined. In *Drosophila*, Cyclin B3 functions redundantly with Cyclin B during mitotic cycles and is required for female meiosis (Jacobs et al., 1998). In *C. elegans*, CYB-3 is required for both mitosis and meiosis (van der Voet et al.,

Development (2016) 143, 3119-3127 doi:10.1242/dev.141226

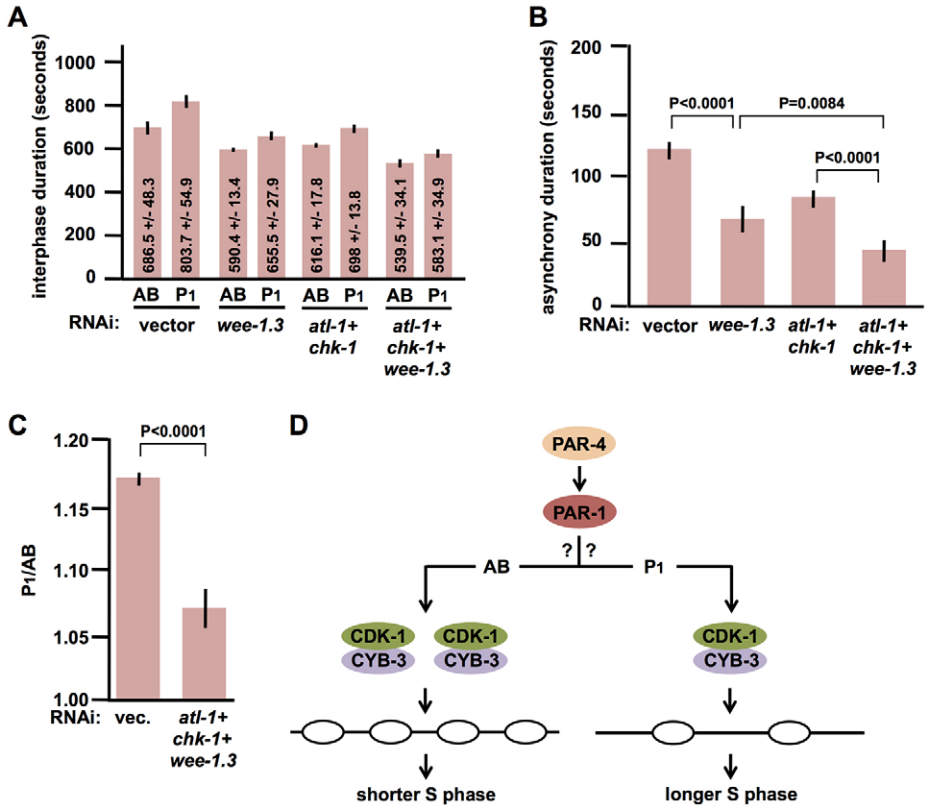

Fig. 6. Inhibitory phosphorylation of CDK-1 is central to the establishment of asynchrony in two-cell embryos. (A) Embryos derived from animals treated with the indicated RNAi(s) were timed for AB and P_1 interphase duration. Ten embryos were timed per sample set. Samples were analyzed in groups of five, the experiment was performed twice, and the values were then combined. (B) Cell cycle asynchrony determined from the data shown in A. (C) P_1/AB ratio for the indicated samples. (A-C) Error bars represent s.d.; *P*-values (where shown) determined by Student's *t*-test. (D) Model of the molecular pathway for cell cycle asynchrony. In this model, PAR-4 and PAR-1 direct asymmetric distribution of CYB-3 through an unknown mechanism (as indicated by the question marks). AB receives more CYB-3 than does P1, and this in turn allows AB to initiate DNA replication more robustly, and to thereby complete S-phase before P1.

2009), while expression studies in mammals point to a meiosis-specific function (Nguyen et al., 2002). Interestingly, loss-of-function analysis has consistently revealed an anaphase function for cyclin B3, as both mitotic and meiotic cell cycles show a metaphase arrest (van der Voet et al., 2009; Deyter et al., 2010; Zhang et al., 2015); however, in some cases the metaphase arrest is dependent on the spindle assembly checkpoint (SAC) (Deyter et al., 2010) whereas in others it is not (Zhang et al., 2015). Even within *C. elegans* the exact role of CYB-3 during mitosis has been difficult to pin down. Genetic experiments support a role for CYB-3 in promoting anaphase by silencing the SAC (Deyter et al., 2010), suggesting that CYB-3 is a negative regulator of the SAC; however, other genetic studies have shown that sterility in SAC mutants is rescued by an increase in *cyb-3* gene dosage (Tarailo-Graovac et al., 2010), suggesting that CYB-3 cooperates with the SAC to ensure faithful chromosome segregation. Furthermore, loss of CYB-3 causes a SAC-dependent delay in progression to anaphase (Deyter et al., 2010), whereas overexpression of CYB-3 also causes an anaphase delay, but in a SAC-independent manner (Tarailo-Graovac and Chen, 2012). As reported here, CYB-3 is required for efficient DNA replication, and thus analysis of mitosis in samples depleted of CYB-3 is complicated by the fact that under-replicated chromosomes may be present. This raises the possibility that some mitotic phenotypes assigned to CYB-3 might be indirect effects of a failure to efficiently replicate the chromosomes in the preceding S-phase.

Asymmetric distribution of CYB-3

Another surprising finding reported here is that CYB-3 is asymmetrically distributed, in a manner dependent on PAR-1 and PAR-4, in two-cell embryos. Interestingly, I also routinely observed that CYB-3 was asymmetrically distributed in the P_1 division products, such that EMS inherited more CYB-3 than its sister P_2 (data not shown), which suggests that an asymmetric distribution of CYB-3 is a general feature of cell division within the P-lineage. PAR-1 and PAR-4 are members of the PAR polarity network that controls numerous aspects of early development, including asymmetric cell division, asynchronous timing, and the asymmetric distribution of cell fate determinants. PAR-1 itself is asymmetrically distributed, with enrichment in the posterior cortex of the one-cell embryo as well as enrichment in P_1 relative to AB, whereas PAR-4 is evenly distributed (Rose and Gönczy, 2014). Work in human cells has shown that PAR-4 (STK11) phosphorylates and activates the kinase activity of PAR-1 (MARK2) (Lizcano et al., 2004), and thus it is possible to model a linear pathway whereby PAR-4 activates PAR-1 to limit the amount of CYB-3 that is inherited by P_1. This type of pathway has been shown to control anterior enrichment of the MEX-5 RNA-binding protein (Griffin et al., 2011); however, MEX-5 asymmetry relies on differential diffusion of the protein within the cytoplasm, a mechanism that is unlikely to apply to CYB-3.

How then might CYB-3 asymmetry be achieved? One possibility is asymmetric distribution of the *cyb-3* mRNA; however, *in situ* hybridization data available in the Nematode Expression Database (NEXTDB; http://nematode.lab.nig.ac.jp) suggest that the *cyb-3* message is evenly distributed in two-cell embryos. Other possibilities include preferential mRNA translation in AB relative to P_1, or enhanced CYB-3 proteolysis in P_1 relative to AB. I favor the second possibility, as existing data show that CYB proteins can be degraded in early embryos by pathways distinct from the canonical anaphase promoting complex (APC) pathway (Liu et al., 2004; Wang et al., 2013). These findings suggest the intriguing possibility that APC-independent pathways for CYB-3 proteolysis might function to promote the asymmetric distribution of CYB-3, and experiments are currently in progress to test this hypothesis.

Development (2016) 143, 3119-3127 doi:10.1242/dev.141226

Another interesting question raised by our work is whether other cyclins are also asymmetrically distributed in early embryos. Previous work has examined this for CYE-1 (cyclin E), and it is evenly distributed (Rivers et al., 2008); however, the intra-embryo distributions of the other CYBs, as well as of CYA-1 (cyclin A), have not been determined.

CYB-3 and S-phase asynchrony

It is well established that cell division within the P-lineage is both asymmetric and asynchronous (Rose and Gönczy, 2014; Tavernier et al., 2015), and that the early cell divisions in the worm embryo are S/M cycles with no gap phases (Edgar and McGhee, 1988). For the two-cell embryo, the length of M-phase is similar between AB and P_1 (Brauchle et al., 2003), whereas the length of S-phase differs, and thus cell cycle asynchrony in the early embryo stems from a difference in the time required to complete DNA replication. How are the differential DNA replication dynamics for AB and P_1 established? Previous work has shown, in early S-phase, that replication is more robust in AB than in P_1 (Benkemoun et al., 2014), suggesting that replication initiates more efficiently in AB. More efficient initiation would allow AB to establish more replication forks in early S-phase, and this would in turn reduce replicon size and thereby allow faster completion of genome duplication. Previous work has also shown that PAR-1 and PAR-4 control replication in the early embryo, through an unknown mechanism, such that these factors repress replication in P_1. In *par-1* and *par-4* mutants, replication is early S-phase is equivalent in two-cell embryos, and the blastomeres then enter mitosis in a synchronous manner (Benkemoun et al., 2014). I have shown here that CYB-3 is required for timely replication, that it is unevenly distributed in a manner dependent on *par-1* and *par-4*, and that it is functionally limiting in P_1 relative to AB. These findings, together with previous work (Benkemoun et al., 2014), suggest a simple model for S-phase asynchrony in which the asymmetric distribution of CYB-3 promotes more efficient replication in AB relative to P_1, thereby allowing AB to complete S-phase before P_1 (Fig. 6D).

Although our data fit well with a differential replication model for cell cycle asynchrony, I note that previous work has identified an alternative possibility with the findings that the G2/M regulators CDC-25.1 and PLK-1 are asymmetrically distributed, in a *par*-dependent manner, in the early embryo (Budirahardja and Gönczy, 2008; Rivers et al., 2008). AB contains more CDC-25.1 and PLK-1 than does P_1, and because these factors positively regulate mitotic entry it has been proposed that this imbalance allows AB to enter mitosis before P_1. Indeed, partial depletion of these factors delays cell cycle progression, and P_1 is more delayed than AB (Budirahardja and Gönczy, 2008; Rivers et al., 2008), which is similar to what I have shown here for CYB-3. While it is clear that CDC-25.1/PLK-1 function is limiting in P_1, it is not known how this would impact S-phase, and given that differential S-phase is the basis for cell cycle asynchrony it remains unclear if the CDC-25.1/PLK-1 asymmetry is itself important for asynchrony. I propose that the CDC-25.1/PLK-1 asymmetry evolved as a way to balance the CYB-3 asymmetry, so that equal ratios of CDK-1–CYB-3 to CDC-25.1/PLK-1 are present in both AB and P_1. This would allow both cells to swiftly enter mitosis once replication has finished. In this scenario, an asymmetric distribution of CYB-3 allows differential DNA replication, and asymmetric distribution of CDC-25.1/PLK-1 ensures that mitotic entry is kinetically similar in AB and P_1.

Although this model is consistent with all available data, further work is needed to unravel how CYB-3 is asymmetrically distributed, and then to experimentally inactivate the asymmetric distribution without disturbing upstream polarity cues. Once this is accomplished, the role of CYB-3 asymmetric distribution in cell cycle asynchrony can be rigorously tested.

MATERIALS AND METHODS

C. elegans maintenance and RNAi

Worms were maintained according to standard procedures (Brenner, 1974). RNAi was performed by feeding (Timmons and Fire, 1998). Details of strains and RNAi conditions are provided in the supplementary Materials and Methods.

Interphase timing of one-cell and two-cell embryos

Gravid adults were placed in a 5 µl drop of M9 on an 18 mm-square coverslip and sliced open with a 20-gauge needle to release embryos. Coverslips were then mounted on microscope slides containing a thin 1.8% agarose pad and embryos were imaged using an Olympus BX51 microscope equipped with DIC optics. Images shown in Fig. 1A, Fig. 2A and Fig. 5A were captured using the 40× objective and a Spot camera (Diagnostic Instruments).

Immunostaining and microscopy

Embryos were permeabilized by freeze-cracking. Details of the antibodies used, including validation, as well as sample fixation, microscopy, image capture and image quantification are provided in the supplementary Materials and Methods.

Acknowledgements

I thank Jean-Claude Labbé for comments on an early draft of this manuscript and Lionel Pintard for helpful discussions.

Competing interests

The author declares no competing or financial interests.

Author contributions

W.M.M. performed all experiments and wrote the manuscript.

Funding

This work was funded by the National Institute of General Medical Sciences, which is part of the National Institutes of Health [R01GM099825 to W.M.M.]. Deposited in PMC for release after 12 months.

Supplementary information

Supplementary information available online at
http://dev.biologists.org/lookup/doi/10.1242/dev.141226.supplemental

References

Benkemoun, L., Descoteaux, C., Chartier, N. T., Pintard, L. and Labbé, J. C. (2014). PAR-4/LKB1 regulates DNA replication during asynchronous division of the early *C. elegans* embryo. *J. Cell Biol.* **205**, 447-455.

Boxem, M., Maliga, Z., Klitgord, N., Li, N., Lemmens, I., Mana, M., de Lichtervelde, L., Mul, J. D., van de Peut, D., Devos, M. et al. (2008). A protein domain-based interactome network for *C. elegans* early embryogenesis. *Cell* **134**, 534-545.

Brauchle, M., Baumer, K. and Gönczy, P. (2003). Differential activation of the DNA replication checkpoint contributes to asynchrony of cell division in *C. elegans* embryos. *Curr. Biol.* **13**, 819-827.

Brenner, S. (1974). The genetics of *Caenorhabditis elegans*. *Genetics* **77**, 71-94.

Budirahardja, Y. and Gönczy, P. (2008). PLK-1 asymmetry contributes to asynchronous cell division of *C. elegans* embryos. *Development* **135**, 1303-1313.

Cowan, C. R. and Hyman, A. A. (2006). Cyclin E-Cdk2 temporally regulates centrosome assembly and establishment of polarity in *Caenorhabditis elegans* embryos. *Nat. Cell Biol.* **8**, 1441-1447.

Deyter, G. M. R., Furuta, T., Kurasawa, Y. and Schumacher, J. M. (2010). *Caenorhabditis elegans* cyclin B3 is required for multiple mitotic processes including alleviation of a spindle checkpoint-dependent block in anaphase chromosome segregation. *PLoS Genet.* **6**, e1001218.

Edgar, L. G. and McGhee, J. D. (1988). DNA synthesis and the control of embryonic gene expression in *C. elegans*. *Cell* **53**, 589-599.

Edgar, L. G., Wolf, N. and Wood, W. B. (1994). Early transcription in *Caenorhabditis elegans* embryos. *Development* **120**, 443-451.
Farrell, J. A., Shermoen, A. W., Yuan, K. and O'Farrell, P. H. (2012). Embryonic onset of late replication requires Cdc25 down-regulation. *Genes Dev.* **26**, 714-725.
Fisher, D. (2011). Control of DNA replication by cyclin-dependent kinases in development. *Results Probl. Cell Differ.* **53**, 201-217.
Fraser, A. G., Kamath, R. S., Zipperlen, P., Martinez-Campos, M., Sohrmann, M. and Ahringer, J. (2000). Functional genomic analysis of *C. elegans* chromosome I by systematic RNA interference. *Nature* **408**, 325-330.
Gallant, P. and Nigg, E. (1994). Identification of a novel vertebrate cyclin: cyclin B3 shares properties with both A- and B-type cyclins. *EMBO J.* **13**, 595-605.
Gönczy, P., Echeverri, C., Oegema, K., Coulson, A., Jones, S. J., Copley, R. R., Duperon, J., Oegema, J., Brehm, M., Cassin, E. et al. (2000). Functional genomic analysis of cell division in *C. elegans* using RNAi of genes on chromosome III. *Nature* **408**, 331-336.
Griffin, E. E., Odde, D. J. and Seydoux, G. (2011). Regulation of the MEX-5 gradient by a spatially segregated kinase/phosphatase cycle. *Cell* **146**, 955-968.
Gunsalus, K. C., Ge, H., Schetter, A. J., Goldberg, D. S., Han, J.-D. J., Hao, T., Berriz, G. F., Bertin, N., Huang, J., Chuang, L.-S. et al. (2005). Predictive models of molecular machines involved in *Caenorhabditis elegans* early embryogenesis. *Nature* **436**, 861-865.
Hachet, V., Canard, C. and Gönczy, P. (2007). Centrosomes promote timely mitotic entry in *C. elegans* embryos. *Dev. Cell* **12**, 531-541.
Jacobs, H. W., Knoblich, J. A. and Lehner, C. F. (1998). *Drosophila* Cyclin B3 is required for female fertility and is dispensable for mitosis like Cyclin B. *Genes Dev.* **12**, 3741-3751.
Ji, J.-Y., Squirrell, J. M. and Schubiger, G. (2004). Both cyclin B levels and DNA-replication checkpoint control the early embryonic mitoses in Drosophila. *Development* **131**, 401-411.
Kamath, R. S., Fraser, A. G., Dong, Y., Poulin, G., Durbin, R., Gotta, M., Kanapin, A., Le Bot, N., Moreno, S., Sohrmann, M. et al. (2003). Systematic functional analysis of the *Caenorhabditis elegans* genome using RNAi. *Nature* **421**, 231-237.
Kemphues, K. J., Priess, J. R., Morton, D. G. and Cheng, N. (1988). Identification of genes required for cytoplasmic localization in early *C. elegans* embryos. *Cell* **52**, 311-320.
Liu, J., Vasudevan, S. and Kipreos, E. T. (2004). CUL-2 and ZYG-11 promote meiotic anaphase II and the proper placement of the anterior-posterior axis in *C. elegans*. *Development* **131**, 3513-3525.
Lizcano, J. M., Göransson, O., Toth, R., Deak, M., Morrice, N. A., Boudeau, J., Hawley, S. A., Udd, L., Mäkelä, T. P., Hardie, D. G. et al. (2004). LKB1 is a master kinase that activates 13 kinases of the AMPK subfamily, including MARK/PAR-1. *EMBO J.* **23**, 833-843.
Lozano, J.-C., Verge, V., Schatt, P., Juengel, J. L. and Peaucellier, G. (2012). Evolution of cyclin B3 shows an abrupt three-fold size increase, due to the extension of a single exon in placental mammals, allowing for new protein-protein interactions. *Mol. Biol. Evol.* **29**, 3855-3871.
McNally, K. L. and McNally, F. J. (2005). Fertilization initiates the transition from anaphase I to metaphase II during female meiosis in *C. elegans*. *Dev. Biol.* **282**, 218-230.
Morton, D. G., Roos, J. M. and Kemphues, K. J. (1992). *par-4*, a gene required for cytoplasmic localization and determination of specific cell types in *Caenorhabditis elegans* embryogenesis. *Genetics* **130**, 771-790.
Nguyen, T. B., Manova, K., Capodieci, P., Lindon, C., Bottega, S., Wang, X.-Y., Refik-Rogers, J., Pines, J., Wolgemuth, D. J. and Koff, A. (2002). Characterization and expression of mammalian cyclin B3, a prepachytene meiotic cyclin. *J. Biol. Chem.* **277**, 41960-41969.
Ortega, S., Prieto, I., Odajima, J., Martín, A., Dubus, P., Sotillo, R., Barbero, J. L., Malumbres, M. and Barbacid, M. (2003). Cyclin-dependent kinase 2 is essential for meiosis but not for mitotic cell division in mice. *Nat. Genet.* **35**, 25-31.
Rabilotta, A., Desrosiers, M. and Labbé, J.-C. (2015). CDK-1 and two B-Type cyclins promote PAR-6 stabilization during polarization of the early *C. elegans* embryo. *PLoS ONE* **10**, e0117656.
Rahman, M. M., Rosu, S., Joseph-Strauss, D. and Cohen-Fix, O. (2014). Down-regulation of tricarboxylic acid (TCA) cycle genes blocks progression through the first mitotic division in *Caenorhabditis elegans* embryos. *Proc. Natl. Acad. Sci. USA* **111**, 2602-2607.
Rivers, D. M., Moreno, S., Abraham, M. and Ahringer, J. (2008). PAR proteins direct asymmetry of the cell cycle regulators Polo-like kinase and Cdc25. *J. Cell Biol.* **180**, 877-885.
Rose, L. and Gönczy, P. (2014). Polarity establishment, asymmetric division and segregation of fate determinants in early *C. elegans* embryos. *WormBook*, 1-43.
Shakes, D. C., Wu, J.-C., Sadler, P. L., LaPrade, K., Moore, L. L., Noritake, A. and Chu, D. S. (2009). Spermatogenesis-specific features of the meiotic program in *Caenorhabditis elegans*. *PLoS Genet.* **5**, e1000611.
Siddiqui, K., On, K. F. and Diffley, J. F. X. (2013). Regulating DNA replication in Eukarya. *Cold Spring Harb. Perspect. Biol.* **5**, a012930.
Sonneville, R., Querenet, M., Craig, A., Gartner, A. and Blow, J. J. (2012). The dynamics of replication licensing in live *Caenorhabditis elegans* embryos. *J. Cell Biol.* **196**, 233-246.
Sonneville, R., Craig, G., Labib, K., Gartner, A. and Blow, J. J. (2015). Both chromosome decondensation and condensation are dependent on DNA replication in *C. elegans* embryos. *Cell Rep.* **12**, 405-417.
Sönnichsen, B., Koski, L. B., Walsh, A., Marschall, P., Neumann, B., Brehm, M., Alleaume, A.-M., Artelt, J., Bettencourt, P., Cassin, E. et al. (2005). Full-genome RNAi profiling of early embryogenesis in *Caenorhabditis elegans*. *Nature* **434**, 462-469.
Tarailo-Graovac, M. and Chen, N. (2012). Proper cyclin B3 dosage is important for precision of metaphase-to-anaphase onset timing in *Caenorhabditis elegans*. *G3* **2**, 865-871.
Tarailo-Graovac, M., Wang, J., Tu, D., Baillie, D. L., Rose, A. M. and Chen, N. (2010). Duplication of *cyb-3* (cyclin B3) suppresses sterility in the absence of mdf-1/MAD1 spindle assembly checkpoint component in *Caenorhabditis elegans*. *Cell Cycle* **9**, 4858-4865.
Tavernier, N., Labbé, J. C. and Pintard, L. (2015). Cell cycle timing regulation during asynchronous divisions of the early *C.elegans* embryo. *Exp. Cell Res.* **337**, 243-248.
Timmons, L. and Fire, A. (1998). Specific interference by ingested dsRNA. *Nature* **395**, 854.
van Der Voet, M., Lorson, M., Srinivasan, D. G., Bennett, K. L. and Van Den Heuvel, S. (2009). *C. elegans* mitotic cyclins have distinct as well as overlapping functions in chromosome segregation. *Cell Cycle* **8**, 4091-4102.
Wang, R., Kaul, Z., Ambardekar, C., Yamamoto, T. G., Kavdia, K., Kodali, K., High, A. A. and Kitagawa, R. (2013). HECT-E3 ligase ETC-1 regulates securin and cyclin B1 cytoplasmic abundance to promote timely anaphase during meiosis in *C. elegans*. *Development* **140**, 2149-2159.
Wieser, S. and Pines, J. (2015). The biochemistry of mitosis. *Cold Spring Harb. Perspect. Biol.* **7**, a015776.
Yan, B., Memar, N., Gallinger, J. and Conradt, B. (2013). Coordination of cell proliferation and cell fate determination by CES-1 Snail. *PLoS Genet.* **9**, e1003884.
Yuan, K. and O'Farrell, P. H. (2015). Cyclin B3 is a mitotic cyclin that promotes the metaphase-anaphase transition. *Curr. Biol.* **25**, 811-816.
Zhang, T., Qi, S.-T., Huang, L., Ma, X.-S., Ouyang, Y.-C., Hou, Y., Shen, W., Schatten, H. and Sun, Q.-Y. (2015). Cyclin B3 controls anaphase onset independent of spindle assembly checkpoint in meiotic oocytes. *Cell Cycle* **14**, 2648-2654.

Supplementary information

Supplemental materials and methods

C. elegans strains

The following strains were used: N2 (wild type), KK184 (*par-4(it47)* V), KK822 (*par-1(zu310)* V), and VC388 (*cyb-3(gk195)* V/nT1 [qIs51] (IV;V). N2 and VC388 were maintained at 20°C, KK184 and KK822 were maintained at 15°C. For temperature shift, KK184 and KK822 young adults were incubated at 24°C for 24 hours. The VC388 strain is balanced by nT1, a reciprocal translocation between linkage groups IV and V. All fertile VC388 progeny are *cyb-3* $^{+/-}$ and these animals produce aneuploid progeny that arrest as embryos or early larvae, fertile *cyb-3*$^{+/-}$ animals, and slow-growing *cyb-3*$^{-/-}$ animals that arrest as L2-L3 larvae (W.M.M., unpublished observations). Arrested embryos and larvae of the *cyb-3*$^{+/+}$ genotype are due to the nT1 balancer translocation.

RNAi

RNAi feeding vectors: feeding vectors against *wee-1.3, atl-1, chk-1,* and *cdk-1* were obtained from the Ahringer feeding library (Source Bioscience). For *cyb-1*, a 534 nt EcoRI-XhoI fragment was isolated from the *cyb-1* cDNA and subcloned into pL4440. This fragment shows 81% identity over a 426 nt stretch to the *cyb-2.1* gene, and 82% identity over a 428 nt stretch to the *cyb-2.2* gene. Using the E-RNAi off-target evaluation software (www.e-rnai.org) it was determined that this RNAi feeding vector could generate 28 21-nt siRNAs against *cyb-2.1* and 24 21-nt siRNAs against *cyb-2.2*, and thus co-depletion of CYB-2.1 and CYB-2.2 with CYB-1 is considered likely. For *cyb-3,* a 1131 nt fragment corresponding to the entirety of the *cyb-3* open reading frame was subcloned into pL4440 as an EcoRI-SalI fragment. This fragment showed no significant identity to any sequences beyond *cyb-3* in the *C. elegans* genome, as inferred by BLAST searches performed on the NCBI database, and no off-target hits were identified using E-RNAi. The resulting plasmids were then transformed into bacterial strain HT115(DE3).

Development • Supplementary information

RNAi conditions: all RNAi was done by feeding and incubation was at 21°C. Standard nematode growth media plates were supplemented with 0.5 mM IPTG and 100 ug/ml carbenicillin. Plates were seeded with overnight cultures of HT115(DE3) transformed with the appropriate feeding vector, as described below, and allowed to dry overnight. Plates were used the following day. For *cyb-1* RNAi, L1-stage animals were plated on *cyb-1* RNAi bacteria and incubated for 60 hours prior to embryo isolation. Under these conditions we observed a high level of embryonic lethality (Fig. S2A), illustrating the efficacy of the RNAi. For *cyb-3* RNAi, L4-stage animals were plated on a mixture of 10% *cyb-3* RNAi bacteria and 90% vector-only (pL4440) bacteria and incubated for 24 hours prior to embryo isolation. For *atl-1/chk-1* RNAi, L1-stage animals were plated on 3:1 mixture of *atl-1* RNAi bacteria and *chk-1* RNAi bacteria and incubated for 36 hours. Animals were then transferred to plates containing 100% vector-only bacteria for an additional 24 hours prior to embryo isolation and timing. For *wee-1.3* RNAi, young adult animals were plated on a mixture of 10% *wee-1.3* RNAi bacteria and 90% vector-only bacteria and incubated for 24 hours prior to embryo isolation and timing. If the time spent on RNAi food was increased, or if the amount of *wee-1.3* RNAi bacteria on the plates was increased, then few if any embryos were produced, owing to defects in oocyte maturation (Burrows et al., 2006). For *atl-1/chk-1/cyb-3* RNAi, L1-stage animals were plated on 3:1 mixture of *atl-1* RNAi bacteria and *chk-1* RNAi bacteria and incubated for 36 hours. Animals were then transferred to plates containing 90% vector-only bacteria and 10% *cyb-3* bacteria for an additional 24 hours prior to embryo isolation and timing.

Antibodies

Mabs F2F4 and K76 were obtained from the Developmental Studies Hybridoma Bank (University of Iowa) and were used at 1:50. P-CDK-1 was detected using antibody sc-7989R (Santa Cruz Biotechnology) diluted at 1:50. PCN-1 was detected using a commercially supplied (Bethyl Laboratories), affinity-purified rabbit antibody raised against a synthetic peptide corresponding to the amino acid sequence N-DIDSEHLGIPDQDYAVVCE-C of *C. elegans* PCN-1.

Development • Supplementary information

Antibody validation

Anti-PCN-1: this antibody recognized a single band of the appropriate size on Western blots of embryo extracts (Fig. S1A).

MabF2F4: Mab F2F4 did not detect a band of any size on Western blots of *C. elegans* embryo extracts (data not shown), suggesting that its antigen in *C. elegans* is not recognized when denatured. Therefore, RNAi was used to deplete embryos of either *cyb-1* or *cyb-3* followed by MabF2F4 staining (Fig. S2B), and this revealed that the MabF2F4 antigen was specifically depleted by *cyb-3* RNAi. As detailed above, the *cyb-1* RNAi used here is likely to also co-deplete *cyb-2.1* and *cyb-2.2*, and thus the signal observed after Mab F2F4 staining of *cyb-1(RNAi)* embryos suggests that Mab F2F4 does not efficiently recognize CYB-1, CYB-2.1, or CYB-2.2. RNAi against both *cyb-1* and *cyb-3* was effective, as evidenced by a high level of embryonic lethality after depletion of either gene (Fig. S2A). To confirm Mab F2F4 cross-reactivity with CYB-3, L2 larvae from strain VC388 were fixed and stained with Mab F2F4 and Mab K76, which recognizes P-granules, and the samples were genotyped by the presence (*cyb-3*$^{+/-}$) or absence (*cyb-3*$^{-/-}$) of pharyngeal GFP signal. As shown in Fig. S2C, *cyb-3*$^{+/-}$ animals displayed a strong Mab F2F4 signal in the developing germline and also in some surrounding somatic nuclei. By contrast, *cyb-3*$^{-/-}$ animals contained just two germ cells, and these were devoid of Mab F2F4 signal (Fig. S2C). Based on the data in Fig. S2, we conclude that Mab F2F4 is specific for CYB-3.

Anti-P-CDK-1: this antibody recognized a single band of the appropriate size on Western blots of embryo extracts (Fig. S3A), and furthermore, anti-P-CDK-1 produced a nuclear signal in control RNAi embryos that was greatly diminished in both *cdk-1(RNAi)* and *wee-1.3(RNAi)* embryos (Fig. S3B).

Immunostaining and image analysis

Antibody staining: embryos were isolated for staining by bleaching young gravid adults. Embryos were spotted on poly-L-lysine coated slides, a coverslip was applied, and the samples were then frozen on dry ice for 10 minutes. The coverslip was then flicked off and the samples processed in one of two ways. For PCN-1, the

Development • Supplementary information

slides were submerged in -20° methanol for one minute. Slides were then transferred to fix solution (1X PBS, 80mM HEPES pH 6.9, 1.6 mM $MgSO_4$, 0.8 mM EGTA, 3.65% formaldehyde) at room temperature for 20 minutes, washed three times in TBS with 0.1% Tween-20 (TBS-T), and blocked for one hour in goat serum. Primary antibodies were applied for either overnight incubation at 4°C or room temperature incubation for two hours. Slides were then washed three times with TBS-T, secondary antibodies were applied, and incubation was carried out at room temperature for 1-2 hours. Slides were then washed three times with TBS-T, mounted in a solution containing DAPI stain, and coverslips were applied and sealed. For MabF2F4 and P-CDK-1 staining, the slides were submerged in -20° methanol for 15 minutes, and then rehydrated in PBS for 5 minutes. Primary antibodies were applied (in PBS) and incubated for 45 minutes at room temperature in a humid box. Slides were washed for 5 minutes in PBS with 0.05% Tween-20 (PBS-T) and then 5 minutes in PBS, then incubated with secondary antibodies for 45 minutes, washed again with PBS-T and then PBS for 5 minutes each, and then mounted in a solution containing DAPI stain, and coverslips were applied and sealed.

Imaging: samples were imaged on an Olympus FLUOVIEW FV1000 confocal laser-scanning microscope. Images (1024x1024 pixel dimensions) were acquired at 40μs/pixel using the 40x objective. Images were not altered after initial capture. For quantification, single optical slices corresponding to maximum CYB-3 signal intensity for AB and P_1 nuclei within a given embryo were quantified for pixel values. For each pair, the AB value was set to 100 and the P_1 value adjusted accordingly. The P_1 values were then averaged.

Supplemental references

Burrows, A.E., Sceurman, B.K., Kosinski, M.E., Richie, C.T., Sadler, P.L., Schumacher, J.M. and Golden, A. (2006). The *C. elegans* Myt1 ortholog is required for the proper timing of oocyte maturation. *Development* **133**, 697–709.

Development • Supplementary information

Sulston, J.E., Schierenberg, E., White, J.G and Thomson, J.N. (1983). The embryonic cell lineage of the nematode *Caenorhabditis elegans*. *Dev. Biol.* **100**, 64–119.

Development • Supplementary information

Figure S1

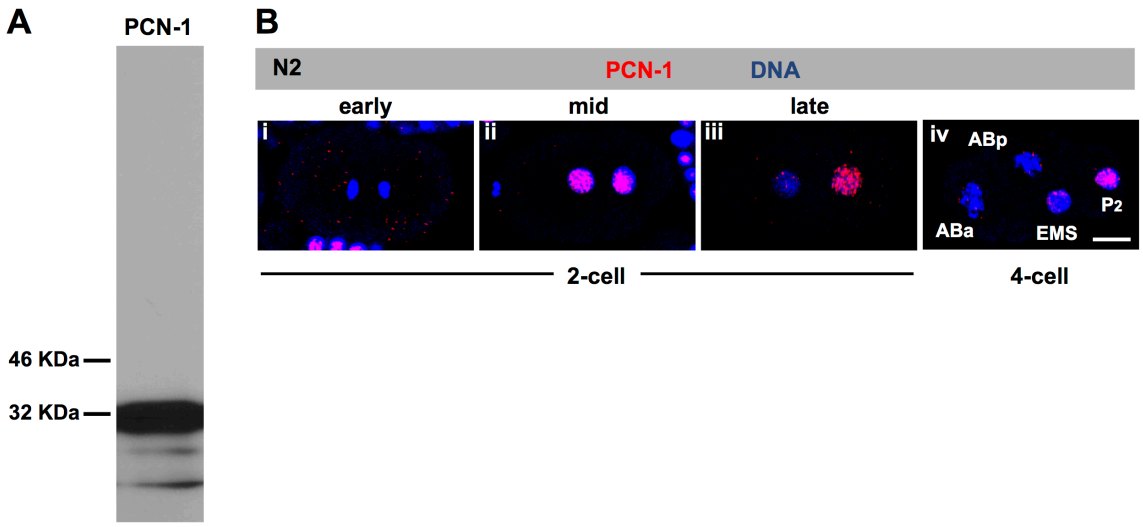

Figure S1. Validation of PCN-1 antibody and confirmation that PCN-1 staining reliably detects replicating nuclei. (A) Embryos were isolated from strain N2 by bleaching, washed, resuspended in SDS-PAGE sample buffer, boiled for 10 minutes, and then loaded on an SDS-PAGE gel. The gel was transferred and probed by Western blotting with anti-PCN-1. (B) Embryos were stained exactly as in Figs 1B-C. Panel i shows an early S-phase embryo that has just begun replication and thus little PCN-1 signal has yet to accumulate. Panel ii shows a later two-cell embryo; note that the PCN-1 signal covers more of the nuclear interior in the anterior AB cell than in P_1. This is consistent with more robust replication in AB during early S-phase (Edgar and McGhee, 1988; Benkemoun et al., 2014). Panel iii shows an older two-cell embryo, where AB has nearly completed S-phase whereas P_1 is still solidly in S-phase. Panel iv shows a four-cell embryo where the P_2 cell is still in S-phase while the other cells are nearly done. This is consistent with P_2 being the last cell to divide amongst the four cells depicted (Sulston et al., 1983). Bar, 10μM.

Development • Supplementary information

Figure S2

A

RNAi	# eggs laid	# eggs hatched
vector	260	260
cyb-1	308	39
cyb-3	279	0

B

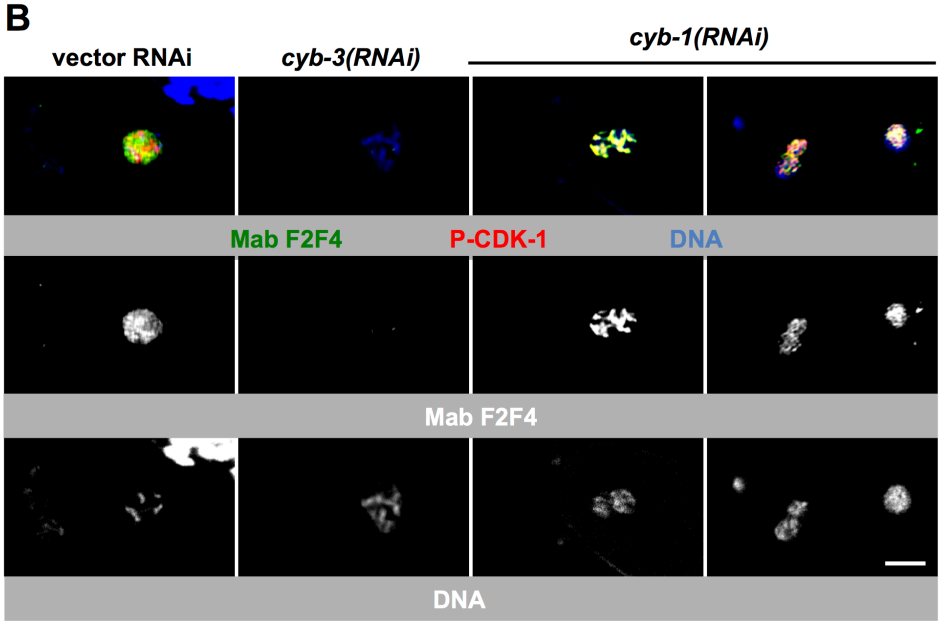

C

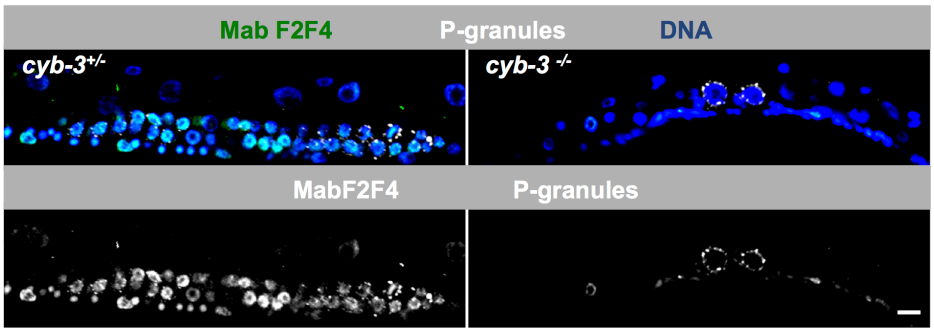

Figure S2. Validation that MabF2F4 specifically recognizes CYB-3. (A) Embryonic lethality after the indicated RNAi. Adults were allowed to lay eggs for 24 hours and then removed. The eggs were counted (# eggs laid) and then counted again 24 hours later to determine the number of eggs that hatched. (B) Animals were treated with the indicated RNAi and embryos were isolated, fixed, and stained with Mab F2F4 (green in top panels), anti-P-CDK-1 (red in top panels), and DAPI

Development • Supplementary information

(DNA, blue in top panels). Bottom panels show uncolored images with the Mab F2F4 and DNA signals alone. For *cyb-1(RNAi)* embryos two samples are shown, one of which shows Mab F2F4 signals in an embryo with multiple nuclei (final set of panels). Bar, 10μM. (C) Stage L2 animals of the indicated genotype were fixed and stained with Mab F2F4 (green in top panels), Mab K76 (P-granules, white in top panels), and DAPI (DNA, blue in top panels). Bottom panels show uncolored images with the Mab F2F4 and K76 signals alone. Bar, 5μM.

Development • Supplementary information

Figure S3

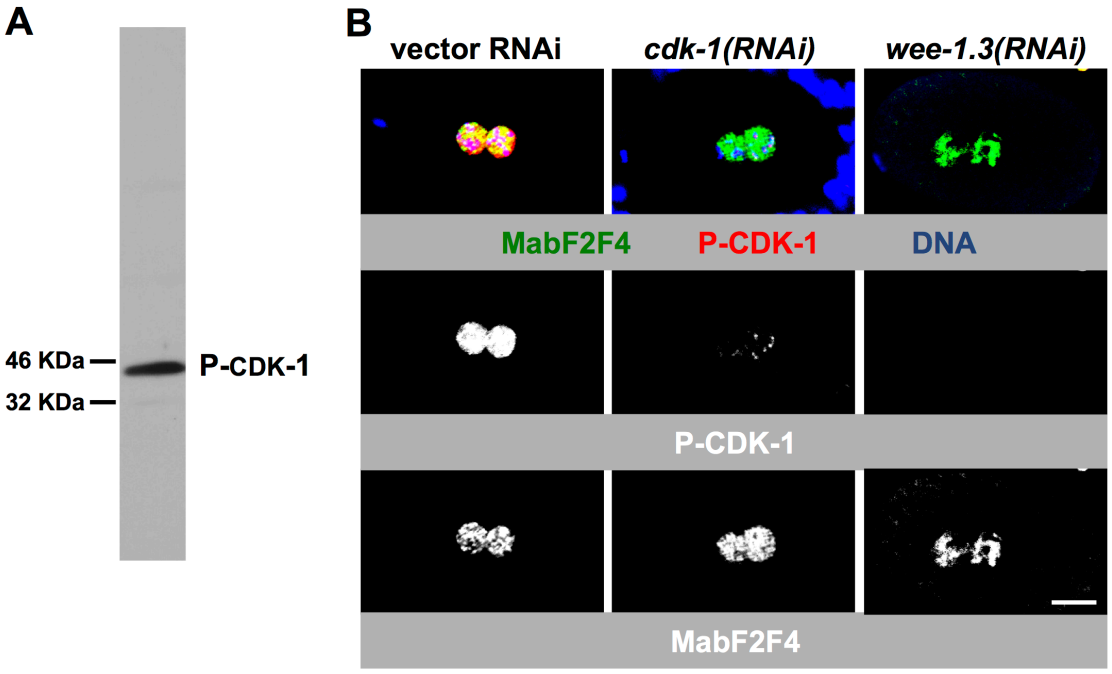

Figure S3. Validation of anti-P-CDK-1 antibody. (A) Embryos were isolated from strain N2 by bleaching, washed, resuspended in SDS-PAGE sample buffer, boiled for 10 minutes, and then loaded on an SDS-PAGE gel. The gel was transferred and probed by Western blotting with anti-P-CDK-1. (B) The indicated RNAi embryos were fixed and stained exactly as in Fig. 3. Bar, 10μM.

Development • Supplementary information